Article

Application of Solid-State ^{35}Cl NMR to the Structural Characterization of Hydrochloride Pharmaceuticals and their Polymorphs

Hiyam Hamaed, Jenna M. Pawlowski, Benjamin F.T. Cooper, Riqiang Fu, S. Holger Eichhorn, and Robert W. Schurko

J. Am. Chem. Soc., **2008**, 130 (33), 11056-11065 • DOI: 10.1021/ja802486q • Publication Date (Web): 26 July 2008

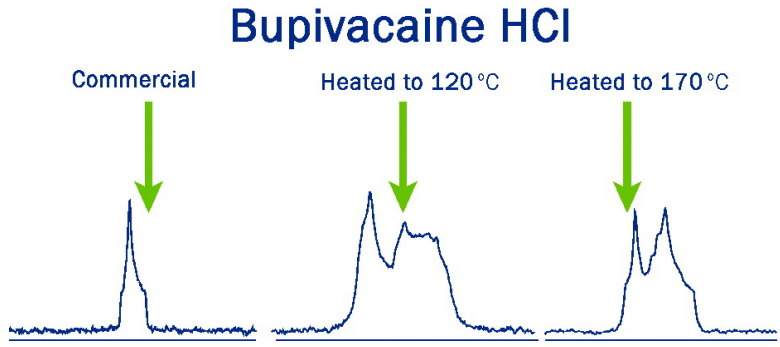

More About This Article

Additional resources and features associated with this article are available within the HTML version:

- Supporting Information
- Access to high resolution figures
- Links to articles and content related to this article
- Copyright permission to reproduce figures and/or text from this article

View the Full Text HTML

J|A|C|S
ARTICLES

Published on Web 07/26/2008

Application of Solid-State ^{35}Cl NMR to the Structural Characterization of Hydrochloride Pharmaceuticals and their Polymorphs

Hiyam Hamaed,[†] Jenna M. Pawlowski,[†] Benjamin F.T. Cooper,[†] Riqiang Fu,[‡] S. Holger Eichhorn,[†] and Robert W. Schurko*,[†]

Department of Chemistry and Biochemistry, University of Windsor, Windsor, Ontario, Canada N9B 3P4 and National High Magnetic Field Laboratory, Tallahassee, Florida 32310-3706

Received April 9, 2008; E-mail: rschurko@uwindsor.ca

Abstract: Solid-state ^{35}Cl NMR (SSNMR) spectroscopy is shown to be a useful probe of structure and polymorphism in HCl pharmaceuticals, which constitute ca. 50% of known pharmaceutical salts. Chlorine NMR spectra, single-crystal and powder X-ray diffraction data, and complementary ab initio calculations are presented for a series of HCl local anesthetic (LA) pharmaceuticals and some of their polymorphs. ^{35}Cl MAS SSNMR spectra acquired at 21.1 T and spectra of stationary samples at 9.4 and 21.1 T allow for extraction of chlorine electric field gradient (EFG) and chemical shift (CS) parameters. The sensitivity of the ^{35}Cl EFG and CS tensors to subtle changes in the chlorine environments is reflected in the ^{35}Cl SSNMR powder patterns. The ^{35}Cl SSNMR spectra are shown to serve as a rapid fingerprint for identifying and distinguishing polymorphs, as well as a useful tool for structural interpretation. First principles calculations of ^{35}Cl EFG and CS tensor parameters are in good agreement with the experimental values. The sensitivity of the chlorine NMR interaction tensor parameters to the chlorine chemical environment and the potential for modeling these sites with ab initio calculations hold much promise for application to polymorph screening for a wide variety of HCl pharmaceuticals.

1. Introduction

Polymorphs, which are distinct, stable phases of a pure substance resulting from a minimum of two different arrangements of the molecules or atoms in the solid state, are of great interest in many areas of chemistry.[1,2] Most active pharmaceutical ingredients (APIs) can adopt more than one polymorphic phase and can also crystallize as pseudopolymorphs, in which the molecules are in distinct hydration or solvation environments. Identification of different polymorphs, or polymorph screening, is of great importance in the pharmaceutical industry and associated laboratories,[3–7] since (i) ca. 80% of solid pharmaceuticals possess more than one polymorphic form[8] and (ii) different polymorphs can have distinct physicochemical properties such as solubility, melting point, dissolution rate, density, hardness, and/or crystal morphology, all of which can affect the bioavailability, handling, packing, shelf life, and/or patenting of a drug.[9–11]

Traditionally, single-crystal and powder X-ray diffraction (XRD) have been the primary methods for solid-state characterization of pharmaceuticals.[12,13] In many cases, isolation of crystals suitable for single-crystal XRD studies is very difficult for standard pharmaceuticals. Powder XRD is useful for distinguishing polymorphs but is often limited for detection of slight structural/conformational changes[14,15] and for providing specific information on the intra- and intermolecular origins of polymorphism. Solid-state nuclear magnetic resonance (SSNMR) experiments are an excellent compliment to XRD methods,[16,17] since they are sensitive to changes in the local electronic environments of nuclei resulting from alterations in molecular structure such as bond length and angle variation, hydrogen bonds, and other intra- and intermolecular interactions.[18–20]

[†] University of Windsor.
[‡] National High Magnetic Field Laboratory.

(1) McCrone, W. C. In *Physics and Chemistry of the Organic Solid State*; Fox, D., Labes, M. M., Weissberger, A., Eds.; Interscience: New York, 1965; Vol. 2, p 725.
(2) Nangia, A. *Acc. Chem. Res.* **2008**, *41*, 595.
(3) Reutzel-Edens, S. M. *Curr. Opin. Drug Discovery Dev.* **2006**, *9*, 806.
(4) Threlfall, T. L. *Analyst* **1995**, *120*, 2435.
(5) Miller, S. P. F.; Raw, A. S.; Yu, L. X. *Polymorphism* **2006**, 385.
(6) Singhal, D.; Curatolo, W. *Adv. Drug Delivery Rev.* **2004**, *56*, 335.
(7) Hilfiker, R.; De Paul, S. M.; Szelagiewicz, M. *Polymorphism* **2006**, 287.
(8) Lohani, S.; Grant, D. J. W. *Polymorphism* **2006**, 21.
(9) Karpinski, P. H. *Chem. Eng. Technol.* **2006**, *29*, 233.
(10) Llinas, A.; Box, K. J.; Burley, J. C.; Glen, R. C.; Goodman, J. M. *J. Appl. Crystallogr.* **2007**, *40*, 379.
(11) Brittain, H. G.; Grant, D. J. W. *Polymorphism in Pharmaceutical Solids*; Marcel Dekker: New York, 1999; Vol. 95, pp 279−330.
(12) Maiwald, M. *Am. Pharm. Rev.* **2006**, *9*, 95.
(13) Brittain, H. G. *Polymorphism in Pharmaceutical Solids*; Marcel Dekker: New York, 1999; Vol. 95, pp 227−278.
(14) Zell, M. T.; Padden, B. E.; Grant, D. J. W.; Schroeder, S. A.; Wachholder, K. L.; Prakash, I.; Munson, E. J. *Tetrahedron* **2000**, *56*, 6603.
(15) Padden, B. E.; Zell, M. T.; Dong, Z.; Schroeder, S. A.; Grant, D. J. W.; Munson, E. J. *Anal. Chem.* **1999**, *71*, 3325.
(16) Harris, R. K. *Analyst* **2006**, *131*, 351.
(17) Berendt, R. T.; Sperger, D. M.; Munson, E. J.; Isbester, P. K. *Trends Anal. Chem.* **2006**, *25*, 977.
(18) Christopher, E. A.; Harris, R. K.; Fletton, R. A. *Solid State Nucl. Magn. Reson.* **1992**, *1*, 93.
(19) Petkova, A. T.; Leapman, R. D.; Guo, Z.; Yau, W.-M.; Mattson, M. P.; Tycko, R. *Science* **2005**, *307*, 262.

 10.1021/ja802486q CCC: $40.75

SSNMR spectroscopy also provides the added benefit of being able to examine disordered or noncrystalline phases of solid pharmaceuticals. In general, ^{13}C SSNMR experiments have been key in probing pharmaceutical polymorphism, allowing for the study of site-specific chemical changes, nonstoichiometric hydration, and solid-state dynamics in heterogeneous and disordered samples, as well as quantification of mixtures of crystalline and/or amorphous forms.[21] In numerous cases where ^{13}C NMR spectra are ambiguous, SSNMR of other nuclides in pharmaceuticals have proven useful, including ^{1}H, ^{2}H, ^{15}N, ^{31}P, ^{19}F, and even ^{23}Na, all of which seem very promising for probing polymorphism.[22–28]

Chlorine SSNMR, to the best of our knowledge, has not been applied for the investigation of pharmaceutical polymorphism, despite the plenitude of hydrochloride (HCl) pharmaceuticals. It is estimated that 50% of all pharmaceutical salts, which are more soluble than nonionic species and extremely useful in solid dosage forms, are HCl pharmaceuticals and that chlorine is present in final formulations of ca. 25% of drugs.[29] It has recently been demonstrated that chlorine NMR is an excellent probe of the Cl^- ion binding environment in HCl amino acids[30,31] and is very useful for distinguishing pseudopolymorphs of chlorine-containing coordination compounds.[32] ^{35}Cl NQR has been applied to study the temperature and phase dependence of ^{35}Cl quadrupolar frequencies in numerous species;[33–35] however, this technique is restricted to systems with larger C_Q's and not generally applicable for $C_Q <$ ca. 10 MHz. Chlorine has two naturally occurring NMR-active nuclides, ^{35}Cl and ^{37}Cl, both of which are half-integer quadrupoles (both spin $^3/_2$, $Q(^{35}\text{Cl}) = -0.082 \times 10^{-28}$ m^2, $Q(^{37}\text{Cl}) = -0.065 \times 10^{-28}$ m^2)[36,37] with low gyromagnetic ratios and are regarded as unreceptive low-gamma nuclei, despite their relatively high natural abundances (75.53% and 24.47%, respectively). The recent increase in the availability of ultrahigh magnetic fields and signal-enhancing pulse sequences has made routine $^{35/37}$Cl SSNMR experimentation a viable option for investigating such systems. Given the sensitivity of the $^{35/37}$Cl quadrupolar interaction to site geometry and chemistry,[30] and the relatively wide chlorine chemical shift range,[38] $^{35/37}$Cl SSNMR should be an excellent probe of structure and polymorphism in HCl pharmaceuticals.

One class of drugs prone to polymorphism is HCl local anesthetics (LAs). LA molecules generally have common structural features which determine their pharmaceutical activities, including a hydrophilic end group, which is normally a tertiary or secondary amine, and a hydrophobic end group, which is usually aromatic.[39] These groups are linked by ester or amide bridges and possess one or more aliphatic chain(s) as substituents.[40] While these structural features allow for conformational flexibility, which undoubtedly influences the drug activity, they also account for the high possibility of polymorph formation.[39,40] The anionic chlorine sites, which adopt unique positions in the unit cell, are expected to have distinct quadrupolar and chemical shift parameters. This suggests that ^{35}Cl NMR spectra can serve as indicators and/or identifiers of different solid phases, providing rapid, unambiguous differentiation of structural polymorphs. Notably, ^{35}Cl SSNMR should find much utility in cases where ^{13}C NMR data are indeterminate or there is a disordered phase(s) unamenable to XRD characterization.

Herein, we report a preliminary study of the application of solid-state ^{35}Cl NMR spectroscopy for the structural characterization of HCl salts of procaine (PH), tetracaine (TH), monohydrated lidocaine (LH), and monohydrated bupivacaine (BH) (Scheme 1) as well as some polymorphs of LH and BH. Quadrupolar and chemical shift parameters extracted from ^{35}Cl SSNMR spectra can be used to distinguish different chlorine environments in these samples; of particular interest is the relationship between the quadrupolar parameters and number of short Cl···H hydrogen bonds. These data are complimented by single-crystal structures, powder XRD patterns, and ^{1}H$-^{13}$C CP/MAS NMR spectra. We hope to demonstrate that the combination of these methods will give us insight into relationships between the structures of the solid pharmaceuticals and their NMR parameters and that ^{35}Cl SSNMR spectroscopy is much needed as a routine screen for polymorphism in pharmaceutical HCl species.

2. Experimental Section

2.1. Sample Preparation and XRD. Samples were purchased from Sigma-Aldrich Canada, Ltd. Crystals of PH were obtained directly from the bottle, whereas crystals of LH, TH, and BH were grown by slow evaporation from acetone, isopropanol, and a solution of water/acetone,[41] respectively. Commercial BH was heated in an oven at 120 °C for 1 day to form polymorph BH1 and was also heated at 170 °C for 12 h using a silicon oil bath to form BH2. Details on the preparation of polymorph LH1 are included in the Supporting Information. Single crystals were covered in Nujol and placed into the cold N_2 stream of a Kryo-Flex low-temperature device. The experiments were performed using the SMART[42] data collection software on a Bruker APEX CCD diffractometer using a graphite monochromator with Mo Kα radiation ($\lambda = 0.710\,73$ Å) source at a temperature of −100 °C. A hemisphere of data was collected using a counting time of 30 s per frame. The data

(20) Byrn, S. R.; Pfeiffer, R. R.; Stephenson, G.; Grant, D. J. W.; Gleason, W. B. *Chem. Mater.* **1994**, *6*, 1148.
(21) Harris, R. K. *J. Pharm. Pharmacol.* **2007**, *59*, 225.
(22) Vogt, F. G.; Brum, J.; Katrincic, L. M.; Flach, A.; Socha, J. M.; Goodman, R. M.; Haltiwanger, R. C. *Cryst. Growth Des.* **2006**, *6*, 2333.
(23) Li, Z. J.; Abramov, Y.; Bordner, J.; Leonard, J.; Medek, A.; Trask, A. V. *J. Am. Chem. Soc.* **2006**, *128*, 8199.
(24) Wawer, I.; Pisklak, M.; Chilmonczyk, Z. *J. Pharm. Biomed. Anal.* **2005**, *38*, 865.
(25) Chupin, V.; De Kroon, A. I. P. M.; De Kruijff, B. *J. Am. Chem. Soc.* **2004**, *126*, 13816.
(26) Smith, E. D. L.; Hammond, R. B.; Jones, M. J.; Roberts, K. J.; Mitchell, J. B. O.; Price, S. L.; Harris, R. K.; Apperley, D. C.; Cherryman, J. C.; Docherty, R. *J. Phys. Chem. B* **2001**, *105*, 5818.
(27) Wenslow, R. M. *Drug Dev. Ind. Pharm.* **2002**, *28*, 555.
(28) Griffin, J. M.; Dave, M. R.; Steven, B. P. *Angew. Chem., Int. Ed.* **2007**, *46*, 8036.
(29) Bighley, L. D. B., S. M.; Monkhouse, D. C. In *Encyclopedia of Pharmaceutical Technology*; Swarbrick, J.,. Boylan, J. C., Eds.; Marcel Dekker: 1995; Vol. 13, p 453.
(30) Bryce, D. L.; Sward, G. D. *J. Phys. Chem. B* **2006**, *110*, 26461.
(31) Bryce, D. L.; Sward, G. D.; Adiga, S. *J. Am. Chem. Soc.* **2006**, *128*, 2121.
(32) Bryce, D. L.; Bultz, E. B. *Chem. Eur. J.* **2007**, *13*, 4786.
(33) Lucken, E. A. C. *Nuclear Quadrupole Coupling Constants*; Academic Press: London, 1969.
(34) Biedenkapp, D.; Weiss, A. *Ber. Bunsen-Ges. Phys. Chem.* **1966**, *70*, 788.
(35) Ramananda, D.; Ramesh, K. P.; Uchil, J. *Magn. Reson. Chem.* **2007**, *45*, 860.
(36) Pyykko, P. *Mol. Phys.* **2001**, *99*, 1617.
(37) Harris, R. K.; Becker, E. D.; Cabral de Menezes, S. M.; Goodfellow, R.; Granger, P. *Solid State Nucl. Magn. Reson.* **2002**, *22*, 458.
(38) Bryce, D. L.; Sward, G. D. *Magn. Reson. Chem.* **2006**, *44*, 409.
(39) Schmidt, A. C.; Niederwanger, V.; Griesser, U. J. *J. Therm. Anal. Calorim.* **2004**, *77*, 639.
(40) Schmidt, A. C.; Senfter, N.; Griesser, U. J. *J. Therm. Anal. Calorim.* **2003**, *73*, 397.
(41) Csoeregh, I. *Acta Crystallogr., Sect. C* **1992**, *C48*, 1794.
(42) *SMART*; Bruker AXS Inc.: Madison, WI, 2001.

Scheme 1. Structures of (a) Procaine HCl (PH), (b) Tetracaine HCl (TH), (c) Lidocaine HCl Monohydrate (LH), and (d) Bupivacaine HCl Monohydrate (BH)

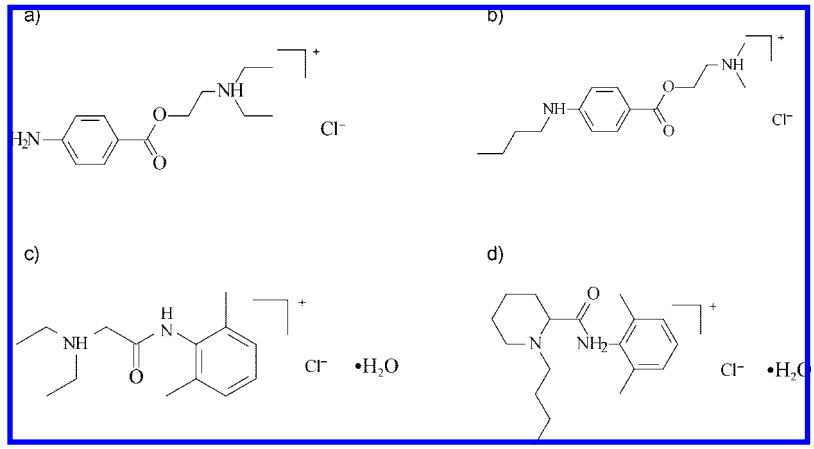

reductions were performed using SAINT,[43] and absorption corrections were applied using SADABS.[44] The structures were solved by direct methods and refined by full-matrix least-squares on F^2 with anisotropic displacement parameters for all non-H atoms using the SHELXL software package.[45] Powder XRD patterns were collected using a D8 DISCOVER X-ray diffractometer equipped with an Oxford Cryosystems 700 Cryostream Plus Cooler. This diffractometer uses a Cu Kα (λ = 1.540 56 Å) radiation source with a Bruker AXS HI-STAR area detector running under the General Area Detector Diffraction System (GADDS).

2.2. Solid-State NMR. ^{35}Cl SSNMR experiments were carried out on a Varian Infinity Plus spectrometer equipped with an Oxford 9.4 T ($\nu_0(^1H)$ = 400 MHz) wide-bore magnet with $\nu_0(^{35}Cl)$ = 39.26 MHz. The ^{35}Cl isotope was chosen instead of ^{37}Cl because of its higher receptivity. High-field ^{35}Cl NMR data were collected on an ultrawide bore 900 MHz (21.1 T) built-in-house superconducting NMR magnet ($\nu_0(^{35}Cl)$ = 88.125 MHz) at the NHMFL in Tallahassee, Florida, as well as on a 900 MHz Bruker Avance II spectrometer at the National Ultrahigh-field NMR Facility for Solids in Ottawa, Canada. All spectra were acquired using the Hahn echo pulse sequence, and chlorine chemical shifts were referenced to NaCl(s) (δ_{iso} = 0.0 ppm), following Bryce and co-workers.[31,38]

2.3. Experiments at 9.4 T. Samples were finely ground and packed into 5 mm o.d. zirconium oxide rotors. ^{35}Cl NMR spectra were collected on a double resonance (HX) static probe. Central-transition selective $\pi/2$ pulse widths between 1.0 and 2.3 μs were applied with an optimized recycle delay of 0.5 s. In cases where NMR powder patterns were too broad to be uniformly excited with a single pulse, spectra were acquired by stepping the transmitter frequency across the entire central transition powder pattern in even increments, collecting individual subspectra and coadding them.[46,47] Experimental times at 9.4 T ranged from 5 to 80 h, depending upon the desired *S*/*N*, pattern breadth, and the number of subspectra collected. Further experimental NMR details can be found in the Supporting Information (Tables S1−S3).

^{1}H−^{13}C CP/MAS NMR spectra of BH and LH were acquired at ν_{rot} = 9.0 and 9.9 kHz, respectively, on a 5 mm HXY probe at 9.4 T. A ^{1}H $\pi/2$ pulse width of 3.25 μs, optimized contact time of 4 ms, recycle delay of 4 s, and ^{1}H decoupling fields of ca. 62 kHz, using the TPPM sequence,[48] were applied. Carbon chemical shifts were referenced with respect to TMS using the high frequency chemical shift of solid adamantane (δ_{iso} = 38.57 ppm) as a secondary reference.

2.4. Experiments at 21.1 T. ^{35}Cl NMR spectra of BH obtained in Ottawa were acquired on a Bruker HX 3.2 mm MAS probe. The ^{35}Cl MAS NMR experiment on BH was performed with a spinning frequency of ν_{rot} = 15 kHz. MAS and static spectra were acquired using selective $\pi/2$ pulse widths of 3.6 and 6.0 μs, respectively, and optimized recycle delays of 1.0 s. The ^{35}Cl MAS NMR experiments conducted at the NHMFL were performed with $\nu_{rot} \approx$ 22 kHz on a built-in-house HX 3.2 mm MAS probe. Selective $\pi/2$ pulse widths of 2.3 or 3.3 μs with ^{1}H decoupling fields of ca. 60 kHz and optimized recycle delays of 1.0 or 2.0 s were employed. For static ^{35}Cl NMR experiments, samples were packed in a rectangular glass container (7.5 × 5 × 11 mm^3), and spectra were acquired on a low-E rectangular-flat coil HX probe.[49] Selective $\pi/2$ pulse widths of ca. 2.0 μs with proton decoupling rf fields of ca. 60.0 kHz were used. Analytical simulations of ^{35}Cl NMR spectra were performed using Wsolids.[50]

2.5. Ab Initio Calculations. ^{35}Cl EFG and CS tensor parameters were calculated using Gaussian 03[51] on Dell Precision workstations and the SHARCNET grid of high performance clusters.[52] Atomic coordinates were input from the crystal structures obtained in our laboratory. All calculations were carried out on clusters comprised of a central chlorine atom and surrounding organic moieties (XYZ coordinates are included with the Supporting Information). Hydrogen atom positions (within 3.6 Å of Cl atoms) were optimized using the B3LYP method,[30] since crystallographic proton positions are estimated during structural refinement. EFG calculations were performed using the Restricted Hartree−Fock (RHF) method with the cc-pVTZ basis set on Cl atoms and cc-pVDZ or 6-31G* basis sets on the other atoms (following Bryce et al.),[30] and with the 6-311+G* basis set on all atoms (for comparison). CS tensor parameters were calculated using the B3LYP method with the aug-cc-pVDZ basis set on the chlorine atom and cc-pVDZ basis set on the other atoms.[30] The nuclear magnetic shielding tensors were calculated using the gauge-including atomic orbitals method

(43) *SAINTPlus*; Bruker AXS Inc.: Madison, WI, 2001.
(44) *SADABS*; Bruker AXS Inc.: Madison, WI, 2001.
(45) Sheldrick, G. M. *SHELXL*, v 6.10 ed.; Bruker AXS Inc.: Madison, WI, 2000.
(46) Medek, A.; Frydman, V.; Frydman, L. *J. Phys. Chem. A* **1999**, *103*, 4830.
(47) Massiot, D.; Farnan, I.; Gautier, N.; Trumeau, D.; Trokiner, A.; Coutures, J. P. *Solid State Nucl. Magn. Reson.* **1995**, *4*, 241.
(48) Bennett, A. E.; Rienstra, C. M.; Auger, M.; Lakshmi, K. V.; Griffin, R. G. *J. Chem. Phys.* **1995**, *103*, 6951.
(49) Gor'kov, P. L.; Chekmenev, E. Y.; Li, C.; Cotten, M.; Buffy, J. J.; Traaseth, N. J.; Veglia, G.; Brey, W. W. *J. Magn. Reson.* **2007**, *185*, 77.
(50) Eichele, K.; Wasylishen, R. E. *WSolids*, 1.17.30 ed., 2001.
(51) Frisch, M. J. et al. Gaussian 03,rev. B.03 ed.; Gaussian, Inc.: Pittsburgh, 2003.
(52) This work was made possible by the facilities of the Shared Hierarchical Academic Research Computing Network (SHARCNET: www.sharcnet.ca).

Table 1. Crystal Structure Data for the HCl Local Anesthetics

	procaine HCl	tetracaine HCl	lidocaine $HCl \cdot H_2O$	bupivacaine $HCl \cdot H_2O$
empirical formula	$C_{13}H_{21}ClN_2O_2$	$C_{15}H_{25}ClN_2O_2$	$C_{14}H_{25}ClN_2O_2$	$C_{18}H_{31}ClN_2O_2$
formula weight (g/mol)	272.77	300.82	288.81	342.90
temperature (K)	173(2)	173(2)	173(2)	173(2)
wavelength (Å)	0.71073	0.71073	0.71073	0.71073
crystal system, space group	orthorhombic, *Pbca*	triclinic, $P\bar{1}$	monoclinic, $P\ 2_1/n$	orthorhombic, *Pbca*
unit cell dimensions				
a (Å)	14.009(2)	7.3436(10)	8.391(2),	18.5429(18)
b (Å)	8.2472(12)	8.5082(12)	7.0150(17)	7.2296(7)
c (Å)	24.853(4)	13.6340(19)	26.163(6)	28.476(3)
α (deg)	90.0	105.5420(10)	90.0	90.0
β (deg)	90.0	91.8630(10)	91.414(3)	90.0
γ (deg)	90.0	99.5810(10)	90.0	90.0
volume (Å^3)	2871.4(7)	806.60(19)	1539.5(6)	3817.4(6)
Z	8	2	4	8
calcd density (g cm^{-3})	1.262	1.239	1.246	1.193
absorption coefficient (mm^{-1})	0.263	0.241	0.249	0.211
$F(000)$	1168	324	624	1488
crystal size (mm^3)	0.3 × 0.2 × 0.2	0.2 × 0.1 × 0.1	0.2 × 0.1 × 0.1	0.2 × 0.1 × 0.1
θ range for data collection (deg)	1.64 to 28.3	2.53 to 28.20	1.56 to 28.27	1.43 to 28.23
limiting indices	$-18 \le h \le 18$, $-10 \le k \le 10$, $-32 \le l \le 32$	$-9 \le h \le 9$, $-10 \le k \le 10$, $-17 \le l \le 17$	$-11 \le h \le 10$, $-9 \le k \le 9$, $-33 \le l \le 33$	$-23 \le h \le 24$, $-9 \le k \le 9$, $-37 \le l \le 37$
reflections collected/unique	30 086/3433 [$R_{(int)} = 0.0447$]	8886/3614 [$R_{(int)} = 0.0268$]	15 806/3503 [$R_{(int)} = 0.1231$]	39 005/4472 [$R_{(int)} = 0.0986$]
refinement method	full-matrix least-squares on F^2			
data/restraints/parameters	3433/0/175	3614/0/189	3503/0/188	4472/0/224
goodness-of-fit on F^2	1.089	1.239	1.457	1.173
final R indices [$I > 2\sigma(I)$][a]	$R_1 = 0.0428$, $wR_2 = 0.1161$	$R_1 = 0.0599$, $wR_2 = 0.1399$	$R_1 = 0.1396$, $wR_2 = 0.2690$	$R_1 = 0.0808$, $wR_2 = 0.1671$
R indices all data	$R_1 = 0.0621$, $wR_2 = 0.1231$	$R_1 = 0.0677$, $wR_2 = 0.1462$	$R_1 = 0.1897$, $wR_2 = 0.2812$	$R_1 = 0.1342$, $wR_2 = 0.1970$
largest diff, peak and hole (e Å^{-3})	0.323 and −0.229	0.317 and −0.372	0.585 and −0.357	0.413 and −0.280

[a] $R1(F) = \Sigma(|F_o| - |F_c|)/\Sigma|F_o|$ for reflections with $F_o > 4(\sigma(F_o))$; $wR2(F^2) = \{\Sigma w(|F_o|^2 - |F_c|^2)^2/\Sigma w|F_o|^2)^2\}^{1/2}$ where w is the weight given for each reflection.

(GIAO).[53,54] The EFG and CS tensor parameters were extracted from the Gaussian output using the EFGShield program.[55]

3. Results and Discussion

3.1. Crystal Structures. Single-crystal X-ray diffraction (XRD) structures of PH[56] and LH,[57] as well as a structure of TH from synchrotron powder XRD data,[58] have previously been reported. Newly refined single-crystal XRD structures for PH, TH, and LH were determined in our laboratory, and we also report the crystal structure for monohydrated bupivacaine (BH). The crystallographic parameters for these samples are listed in Table 1, and partial crystal structures are shown in Figure 1. Powder XRD patterns were obtained for all four parent samples and found to match very well with simulated powder XRD patterns, ensuring the purity of the bulk samples (Figures S1−S4, Supporting Information). Structural features of these systems will be addressed in the NMR discussion below.

3.2. Solid-State ^{35}Cl NMR. In this section, solid-state ^{35}Cl NMR spectra of the four parent compounds, as well as polymorphs of LH and BH, will be discussed. All solid-state ^{35}Cl NMR spectra and associated simulations are shown in Figures 2 and 3, and the parameters are summarized in Table 2. Magic-angle spinning (MAS) NMR spectra were acquired at 21.1 T, in order to separate the partially averaged, second-order quadrupolar-dominated central transition from the spinning sidebands, thereby allowing for the accurate determination of the quadrupolar coupling constants, C_Q, asymmetry parameters, η_Q, and isotropic chemical shifts, δ_{iso} (see Table 2 for definitions and conventions; detailed background discussion on ^{35}Cl SSNMR can be found in ref 38). Static ^{35}Cl NMR spectra were acquired at both 9.4 and 21.1 T, in order to deconvolute spectral contributions from the electric field gradient (EFG) and chemical shielding (CS) tensors and to extract the anisotropic chlorine CS parameters.

3.2.1. PH and TH. PH has been recrystallized from a variety of solvents and stored at high humidity, but no polymorphic forms have been observed.[59] TH, unlike PH, is known to form polymorphs arising from either heating or different recrystallization processes.[59] However, for the purpose of this work, PH and TH polymorphism will not be discussed further; rather, these compounds will serve as benchmarks for comparison of ^{35}Cl NMR parameters with structural data for HCl LA salts and other analogous chlorine-containing systems.

(53) Ditchfield, R. *Mol. Phys.* **1974**, *27*, 789.
(54) Wolinski, K.; Hinton, J. F.; Pulay, P. *J. Am. Chem. Soc.* **1990**, *112*, 8251.
(55) Adiga, S.; Aebi, D.; Bryce, D. L. *Can. J. Chem.* **2007**, *85*, 496.
(56) Dexter, D. D. *Acta Crystallogr., Sect. B* **1972**, *28*, 77.
(57) Hanson, A. W.; Roehrl, M. *Acta Crystallogr., Sect. B* **1972**, *28*, 3567.
(58) Nowell, H.; Attfield, J. P.; Cole, J. C.; Cox, P. J.; Shankland, K.; Maginn, S. J.; Motherwell, W. D. S. *New J. Chem.* **2002**, *26*, 469.
(59) Giron, D.; Draghi, M.; Goldbronn, C.; Pfeffer, S.; Piechon, P. *J. Therm. Anal.* **1997**, *49*, 913.

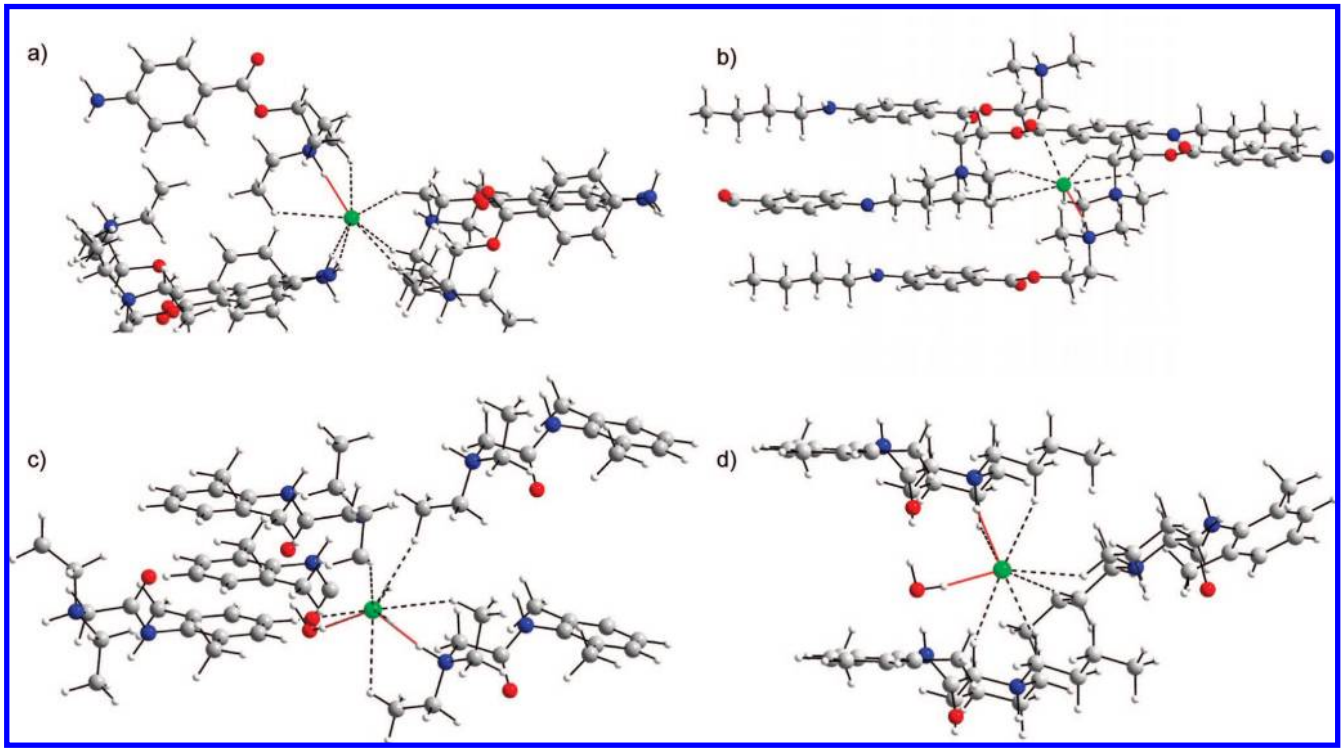

Figure 1. Partial crystal structures of (a) PH, (b) TH, (c) LH, and (d) BH, which focus on the chlorine atom positions. The short chlorine−hydrogen contacts are indicated in red, and longer contacts are marked with dashed lines. For TH and LH, some atoms are deleted for clarity.

According to our single crystal X-ray structure of PH (Figure 1a), there is one crystallographic Cl site with a close Cl···HN contact of 2.150 Å and seven longer Cl···H contacts between 2.545 and 3.087 Å, similar to the previously reported structure.[52] ^{35}Cl NMR spectra (Figure 2a) show powder patterns corresponding to a single Cl site with parameters similar to those of cocaine HCl (C_Q = 5.027 MHz, η_Q = 0.2)[60] and quinuclidine HCl (C_Q = 5.25 MHz, η_Q = 0.05).[61] Both have chlorine environments similar to that of PH, with each Cl surrounded by eight H atoms, and single close contacts (Cl···HN = 2.098 and 1.888 Å, respectively).[62]

A crystal structure of TH was obtained in our laboratory after recrystallization of commercial TH from isopropanol (Figure 1b). This new structure is similar to a previously reported one[58] and has a single short Cl···HN contact of 2.112 Å and six longer Cl···HC contacts ranging from 2.794 to 3.044 Å. ^{35}Cl NMR spectra of TH (Figure 2b) reveal similar NMR parameters to those of PH. The slightly larger C_Q for TH is consistent with its shorter Cl···HN contact; clearly, short, single Cl···H contacts dominate the magnitude of V_{33}, the largest component of the EFG tensor.[31] For both PH and TH, static NMR spectra acquired at 21.1 T allow for refinement of the quadrupolar parameters, as well as the determination of the principal components of the chlorine CS tensors and the relative orientation of the CS and EFG tensors (Table 2). The chlorine chemical shift anisotropy (CSA) parameters are in the range of those reported in the literature for similar systems.[38]

3.2.2. LH and Polymorph LH1. The crystal structure of LH determined in our laboratory (Figure 1c) is different from that previously reported;[57] however, they both have only one chlorine site in the asymmetric unit. The Cl^- ion in our structure has two hydrogen bonds (Cl···H = 2.206 and 2.402 Å) and seven more distant Cl···H contacts (ranging from 2.7 to 3.1 Å). ^{35}Cl NMR spectra (Figure 2c) of this sample reveal a value of C_Q close to that of PH; however, the η_Q is distinct from those of PH and TH. The higher η_Q for LH indicates a reduction in the axial symmetry of the ^{35}Cl EFG tensor, which possibly results from the presence of two short Cl···H contacts, as opposed to the single contacts in PH and TH.

It is well known that the presence of coordinating or noncoordinating water molecules can influence the solid-state structures of hydrated pharmaceutical solids.[22,63,64] There have been no other reports of LH polymorphs; nevertheless, a new form (LH1) was made in our laboratory (Supporting Information). Thermal gravimetric analysis (TGA) and solution ^{1}H NMR experiments confirm that both the commercial LH and LH1 samples are monohydrates. TGA curves (Figure S5) show that the water molecules are lost at different temperatures (at 65 °C for LH and 50 °C for LH1), implying structural differences between these forms. LH1 has a distinct powder XRD pattern from LH, but a crystal suitable for single-crystal XRD could not be obtained. The ^{1}H−^{13}C CP/MAS NMR spectra are slightly different, with similar groupings of peaks on a coarse chemical shift scale but clear distinctions on a finer scale. While this data combination is indicative of polymorphism, little insight into the actual differences between LH and LH1 is readily available.

On the other hand, the ^{35}Cl NMR spectra of LH1 reveal two overlapping second-order patterns, which are especially apparent in the static spectra (Figures 2d and S6). These spectra indicate

(60) Yesinowski, J. P.; Buess, M. L.; Garroway, A. N.; Ziegeweid, M.; Pines, A. *Anal. Chem.* **1995**, *67*, 2256.
(61) Bryce, D. L.; Gee, M.; Wasylishen, R. E. *J. Phys. Chem. A* **2001**, *105*, 10413.
(62) Zhu, N.; Harrison, A.; Trudell, M. L.; Klein-Stevens, C. L. *Struct. Chem.* **1999**, *10*, 91.
(63) Lester, C.; Lubey, G.; Dicks, M.; Andol, G.; Vaughn, D.; Cambron, R. T.; Poiesz, K.; Redman-Furey, N. *J. Pharm. Sci.* **2006**, *95*, 2631.
(64) Vogt, F. G.; Dell'Orco, P. C.; Diederich, A. M.; Su, Q.; Wood, J. L.; Zuber, G. E.; Katrincic, L. M.; Mueller, R. L.; Busby, D. J.; DeBrosse, C. W. *J. Pharm. Biomed. Anal.* **2006**, *40*, 1080.

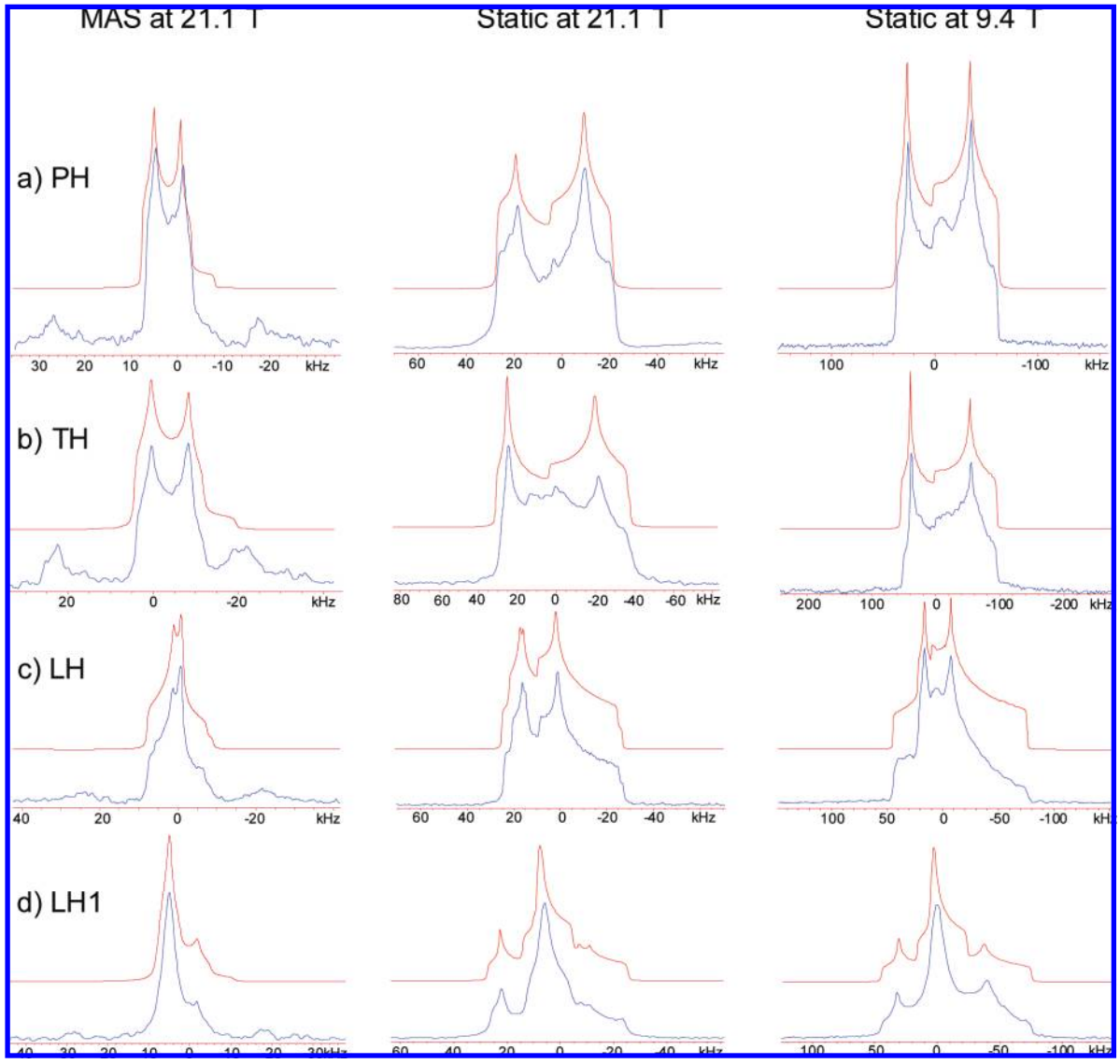

Figure 2. ^{35}Cl SSNMR spectra (bottom) and simulations (top) of (a) PH, (b) TH, (c) LH, and (d) polymorph LH1.

the presence of two chlorine environments with quadrupolar parameters distinct from that of LH. Site 1, which is distinguished by a narrower central pattern, has a small C_Q, a high η_Q, and a small span, all of which are similar to analogous parameters reported for L-cysteine methyl ester HCl,[61] which has a Cl^- ion with three short Cl···HN contacts (ranging between 2.256 and 2.389 Å).[65] Site 2 has a broad pattern with two clearly visible discontinuities, arising from a larger C_Q and η_Q closer to zero as well as a slightly larger span. These values are similar to those measured for PH, TH, and quinuclidine HCl,[61] all of which have a Cl^- ion with only one short Cl···H contact, suggesting that site 2 is of a similar nature. The identification of these two structurally unique Cl sites confirms that LH and LH1 are polymorphs and intimates two possibilities: (i) LH1 is a single phase with two crystallographically distinct Cl sites or (ii) LH1 is a mixture of two phases, each with a crystallographically distinct Cl site; the TGA data suggest that the former is highly probable. Information obtained from ^{35}Cl SSNMR in this case is invaluable in considering options for refinement of powder XRD data, additional ^{13}C and ^{1}H NMR experiments, etc., for further polymorph characterization; of course, full discussion of this complete characterization is beyond the scope of the current work.

3.2.3. BH and Polymorphs BH1 and BH2. The crystal structure of anhydrous BH has been reported in the literature;[41] however, the commercial BH is monohydrate. Recrystallization of the commercial BH, and ensuing refinement of single-crystal XRD data, reveals a single chlorine site with two hydrogen bonds (Cl···HO = 2.106 Å and Cl···HN = 2.374 Å) and six other Cl···HC contacts ranging between 2.835 and 3.045 Å. ^{35}Cl SSNMR spectra of BH (Figure 3a) reveal a smaller C_Q and a higher η_Q than those of the LAs discussed above. The Cl···HN contact in BH is the longest of the four pharmaceuticals, and the Cl···HO contact is short by comparison. As a result, the quadrupolar parameters for BH are extremely different from the complexes discussed thus far, with V_{33} no longer dominated by a short Cl···HN contact.

(65) Gorbitz, C. H. *Acta Chem. Scand.* **1989**, *43*, 871.

(66) Lubach, J. W.; Padden, B. E.; Winslow, S. L.; Salsbury, J. S.; Masters, D. B.; Topp, E. M.; Munson, E. J. *Anal. Bioanal. Chem.* **2004**, *378*, 1504.

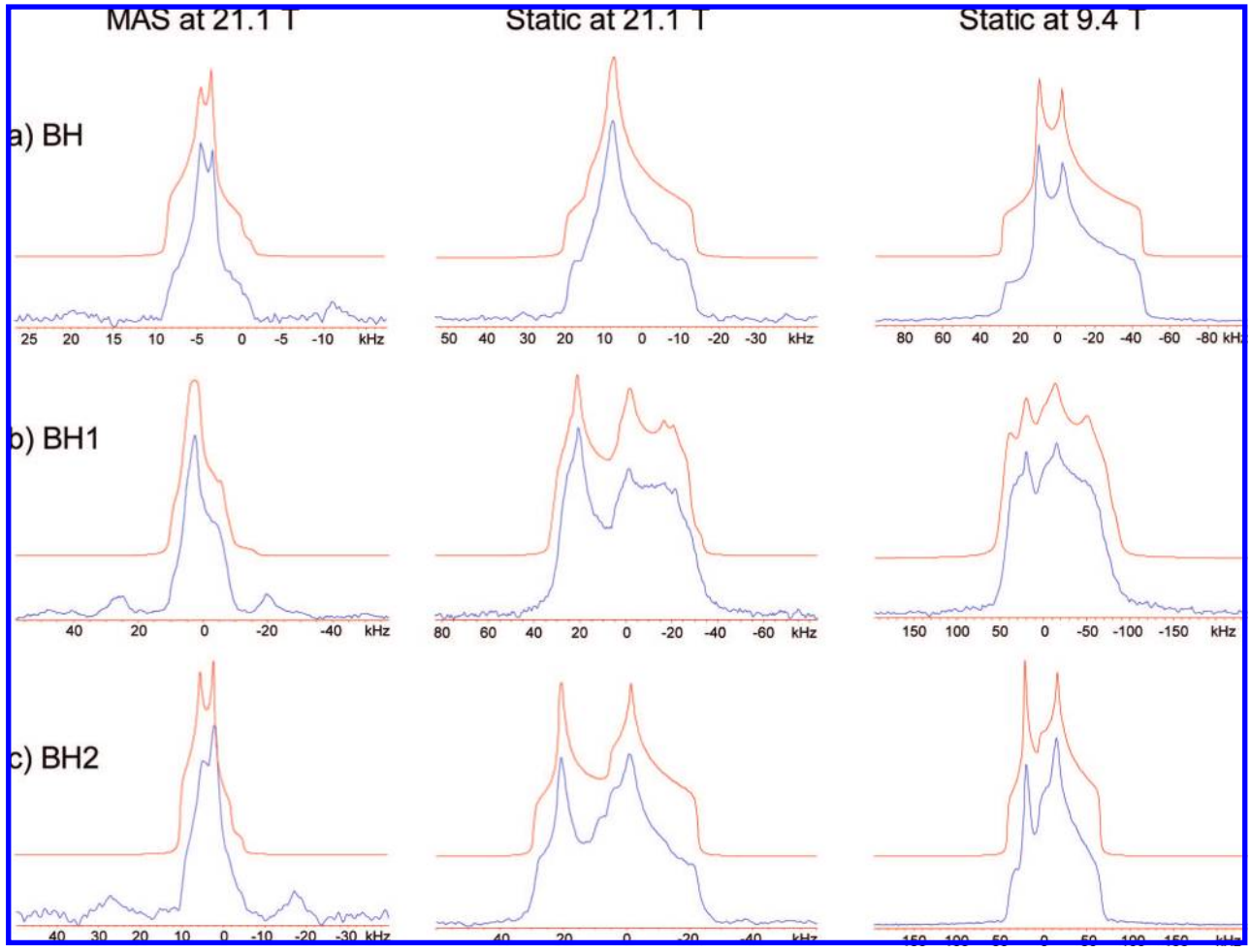

Figure 3. ^{35}Cl SSNMR spectra (bottom) and simulations (top) of monohydrated bupivacaine HCl (BH) and its polymorphs: (a) commercial BH; (b) BH1 is a polymorph obtained from BH by heating it to 120 °C; (c) BH2 is a polymorph obtained from BH by heating it to 170 °C.

Table 2. Summary of the Experimental ^{35}Cl NMR Parameters

	C_Q/MHz[a]	η_Q[b]	δ_{iso}/ppm[c]	δ/ppm[d]	κ[e]	α/deg	β/deg	γ/deg
PH	4.87(7)	0.28(4)	96(6)	125(25)	−0.4(3)	95(15)	3(2)	32(8)
TH	6.00(10)	0.27(4)	71(6)	80(15)	0.4(3)	60(8)	8(5)	10(10)
LH	4.67(7)	0.77(3)	100(4)	110(15)	−0.85(3)	12(3)	40(10)	80(3)
LH1 site 1	2.52(12)	0.95(5)	85(10)	20(10)	−0.8(2)	90(40)	50(50)	60(40)
LH1 site 2	5.32(10)	0.32(10)	110(10)	45(10)	0.8(2)	5(5)	50(15)	40(40)
BH	3.66(10)	0.72(8)	96(10)	100(25)	0.2(4)	105(20)	90(5)	5(5)
BH1 site 1	4.75(20)	0.65(10)	118(10)	160(40)	0.9(1)	10(10)	3(1)	0(2)
BH1 site 2	5.85(20)	0.26(4)	95(10)	160(40)	−0.2(1)	18(4)	50(5)	80(5)
BH2	4.58(5)	0.56(6)	118(5)	120(10)	0.8(1)	10(10)	0(2)	50(50)

[a] Theoretical values of C_Q ($C_Q = eQV_{33}/h$) are calculated by converting from atomic units to Hz by multiplying V_{33} by $(eQ/h)(9.7177 \times 10^{21}$ V $m^{-2})$, where $Q(^{35}Cl) = -0.082 \times 10^{-28}$ m^2. [b] $\eta_Q = (V_{11} - V_{22})/V_{33}$. [c] $\delta_{iso} = (\delta_{11} + \delta_{22} + \delta_{33})/3$. [d] $\Omega = \delta_{11} - \delta_{33}$. [e] $\kappa = 3(\delta_{22} - \delta_{iso})/\Omega$.

BH is known to form polymorphs when heated or solvates when recrystallized from different solvents.[66] Heating the BH sample to 120 °C leads to the formation of a polymorph, BH1, whose structure is unknown. The ^{35}Cl NMR spectra indicate the presence of two distinct chlorine sites with environments different than those in the commercial BH (Figure 3b and S7). In addition, the spectral discontinuities are not as sharp as those in NMR spectra of highly crystalline samples, indicating some degree of disorder. However, the fact that discontinuities are observed at all is consistent with some crystallinity, as confirmed by the corresponding powder XRD patterns and ^{13}C NMR data acquired by us (Figure 5) and others.[66] Both sites have larger quadrupolar interactions than that of BH: site 1 (C_Q = 4.75 MHz) is similar to the chlorine site in LH (two Cl ···H bonds), whereas site 2 (C_Q = 5.85 MHz) indicates a coordination environment similar to that in TH (one Cl ···H bond).

Heating the BH sample to 170 °C leads to the formation of another crystalline polymorph, BH2.[66] Comparisons of powder XRD patterns and ^{13}C NMR spectra (Figure 5) of BH1 and BH2 indicate subtle differences between the two samples but are inconclusive with regard to polymorphism and are not particularly useful for any structural interpretation. However, ^{35}Cl NMR data (Figure 3c) indicate that BH2 has only one chlorine site, with quadrupolar parameters that are similar to site 1 of BH1. In addition, the discontinuities in the ^{35}Cl NMR powder patterns of BH2 are sharper than those of BH1, consistent with indications of higher crystallinity of BH2 indicated by both sharper powder XRD peaks (Figure S4) and

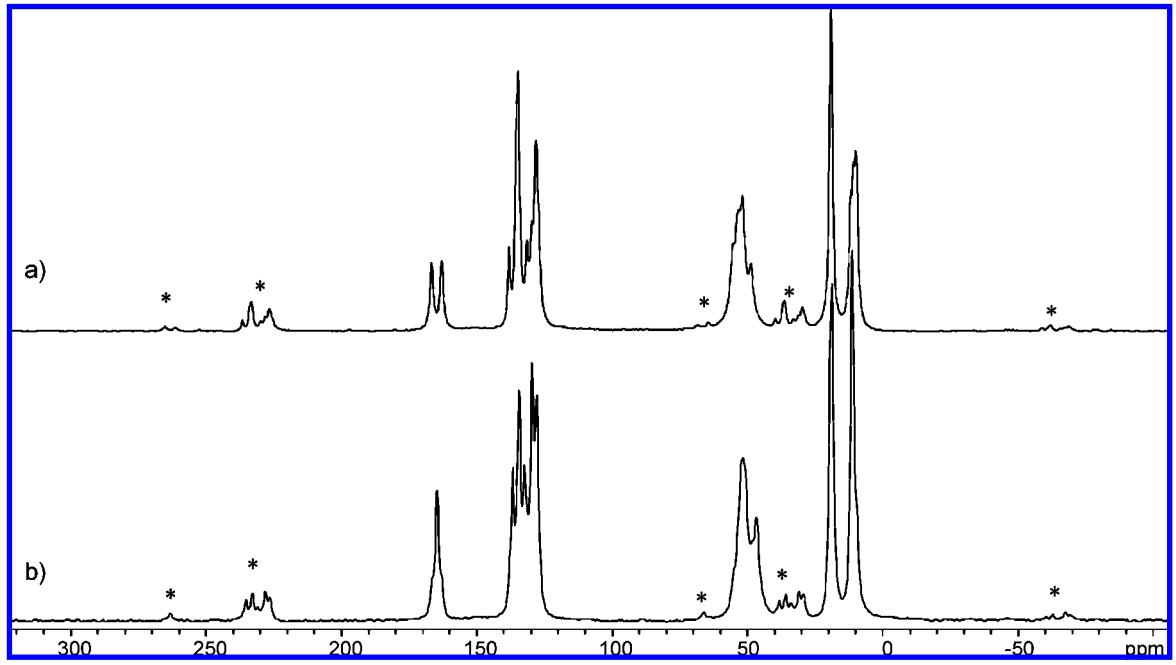

Figure 4. ^{13}C NMR of the monohydrated lidocaine hydrochloride (LH) samples acquired at $B_0 = 9.4$ T, $\nu_{rot} = 9.9$ kHz: (a) polymorph LH1, (b) commercial LH. LH has one molecule per asymmetric unit, while LH1 has two molecules per asymmetric unit, as clearly seen in the splitting of the chemical shift of the carbonyl group (165 ppm). *: denote spinning sidebands.

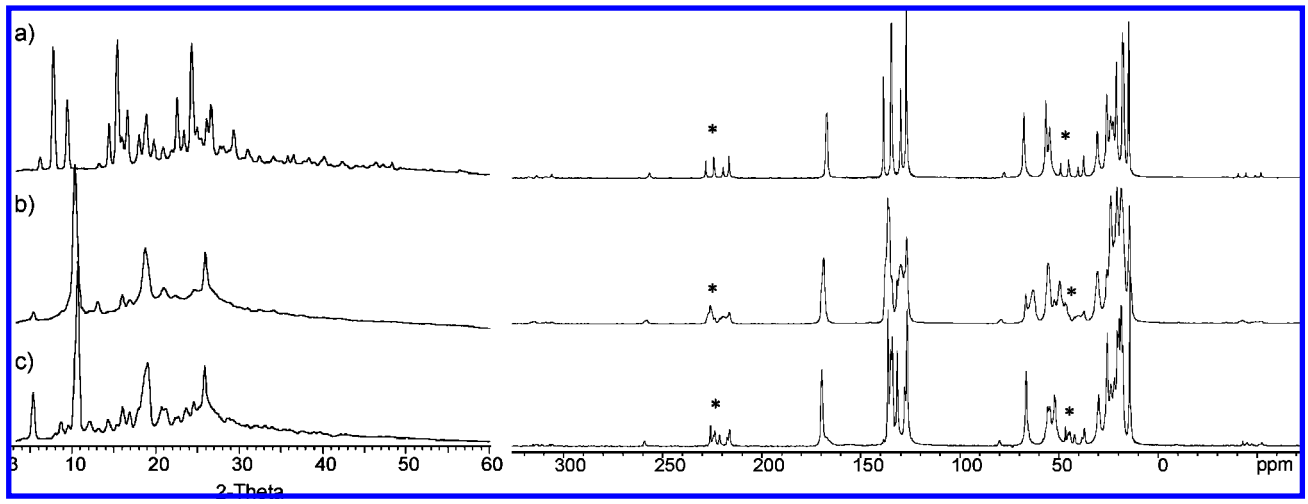

Figure 5. Powder XRD (left) and ^{13}C NMR spectra (right) acquired at 9.4 T, $\nu_{rot} = 9.0$ kHz: (a) commercial BH, (b) polymorph BH1 (heated to 120 °C), (c) polymorph BH2 (heated to 170 °C). *: denote spinning sidebands.

^{13}C NMR peaks (Figure 5). In comparing ^{35}Cl NMR data for BH1 and BH2, it is surmised that (i) BH1 is a mixture of a noncrystalline phase with one type of chlorine environment and a crystalline phase with a second distinct chlorine environment and (ii) BH2 is comprised solely of one crystalline phase. Therefore, heating from room temperature to 120 °C produces new crystalline and disordered phases in BH1, the latter of which is detected by ^{35}Cl NMR but not by powder XRD. The disordered phase disappears after heating to 170 °C, leaving only a unique crystalline phase, BH2, which is similar but not identical to the crystalline phase in BH1. In this instance, the ^{35}Cl NMR data are crucial in demonstrating that BH1 and BH2 are distinct polymorphs and reveal a phase undetectable by XRD techniques.

3.3. Theoretically Calculated NMR Interaction Tensors. An appreciation of the relationships between solid-state structures and chlorine NMR interaction tensors will be crucial for making future structural interpretations for the many HCl pharmaceuticals for which crystal structures are unavailable. To develop a basis for understanding these relationships, we have conducted ab initio calculations of the ^{35}Cl EFG and CS tensors of the four parent pharmaceuticals and carefully examined the principal components and tensor orientations with respect to the molecular coordinates. Following the work of Bryce et al.,[30] RHF calculations were found to provide the closest agreement with experiment for EFG tensor parameters, and B3LYP calculations were considerably better for CS tensor parameters (full details on the basis sets and construction of the individual molecular coordinate systems are given in the Experimental Section and Supporting Information, with key results summarized in Tables 3 and S4). In all calculations, the molecular coordinates were taken from single-crystal structures, and only proton positions were geometry optimized.

Table 3. Comparison of the Experimental and Theoretical ^{35}Cl EFG and CS Tensor Parameters[a,b]

	C_Q/MHz	η_Q	δ_{iso}/ppm	Ω/ppm	κ	α/deg	β/deg	γ/deg
PH exptl	4.87(7)	0.28(4)	96(6)	125(25)	−0.4(3)	95(15)	3(2)	32(8)
PH calcd	−5.41	0.286	96	114.4	−0.16	21	6	72
TH exptl	6.0(1)	0.27(4)	71(6)	80(15)	0.4(3)	60(8)	8(5)	10(10)
TH calcd	−6.11	0.20	105	103.4	0.49	51	31	57
LH exptl	4.67(7)	0.77(3)	100(4)	110(15)	−0.85(3)	12(3)	40(10)	80(3)
LH calcd	−4.097	0.437	120	115.05	−0.52	50	78	75
BH exptl	3.66(10)	0.72(8)	96(10)	100(25)	0.2(4)	105(20)	90(5)	5(5)
BH calcd	3.91	0.84	108	117.24	−0.1	164	85	4.2

[a] Definitions of parameters are given in Table 1. [b] All theoretical EFG parameters are obtained from RHF calculations featuring cc-PVTZ on the Cl atoms and 6-31G* on all other atoms. Other calculations producing reasonable agreement with experiment are included in the Supporting Information.

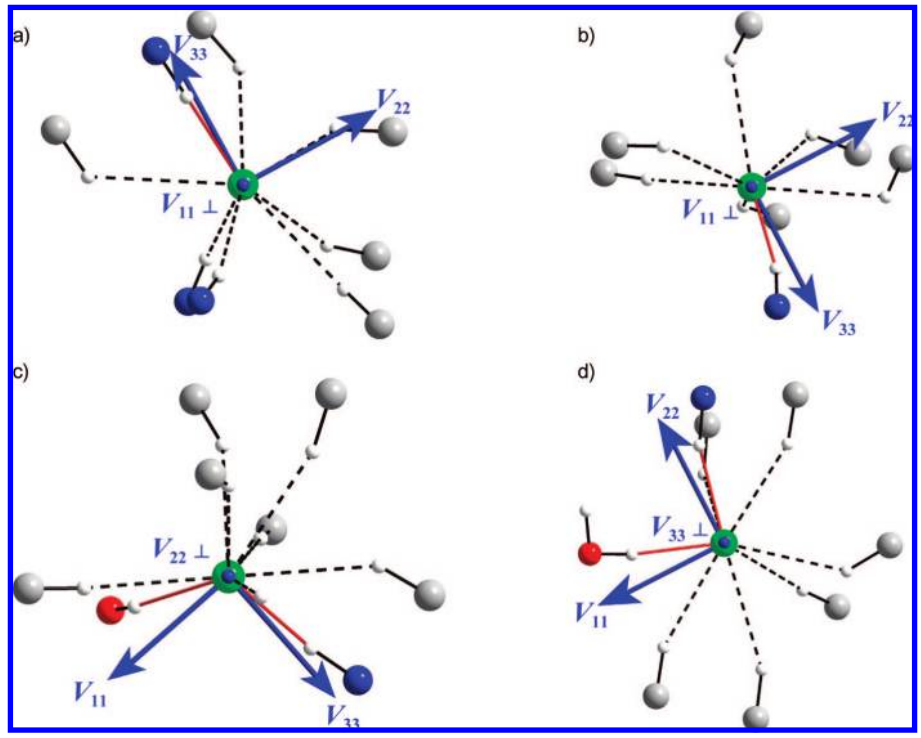

Figure 6. ^{35}Cl EFG tensor orientations in (a) PH, (b) TH, (c) LH, and (d) BH. The diagrams above are magnifications of the chlorine sites pictured in Figure 1.

In general, the agreement between the experimental and theoretical ^{35}Cl EFG parameters is quite good, with the only significant discrepancy being the values of η_Q for LH (exptl 0.77, theor 0.44). It is instructive at this point to consider the EFG tensor orientations and local atomic coordinates to understand the origins of the ^{35}Cl quadrupolar parameters. PH and TH, as noted earlier, both feature single, short Cl···HN contacts, with the shorter contact distance corresponding to the larger value of C_Q in TH. Visualization of the tensor orientation aids in understanding these EFG parameters: in each case, V_{33} is found to be oriented close to the Cl···HN bond axis ($\angle(V_{33}-\text{Cl}-\text{H}) = 4.6°$ and 24.8°, in PH and TH, respectively), accounting for its dependence on contact length (Figure 6a, 6b). Since there are no other short contacts, V_{11} and V_{22} are similar to one another, and the value of η_Q is closer to zero than to 1.

LH and BH both possess two short hydrogen-bonding contacts: Cl···HN and Cl···HO. These environments are distinct from those of PH and TH, as reflected in the higher values of η_Q. For LH, V_{33} is again oriented very near to the Cl···HN bond axis (Figure 6c, $\angle(V_{33}-\text{Cl}-\text{H}) = 11.6°$), and the r(Cl···H) is very similar to that in PH, accounting for their similar values of C_Q. However, V_{11} and V_{22} are differentiated from one another by the presence of the short Cl···HO contact with an H_2O molecule. Rapid motion of the H_2O molecule and variation in proton coordinates very likely account for the discrepancy between experimental and theoretical values of η_Q. The Cl···HN contact in BH is the longest of the four pharmaceuticals (2.374 Å, geom. opt. 2.182 Å), and the Cl···HO contact is short by comparison (2.106 Å, geom. opt. 2.087 Å). As a result, the ^{35}Cl EFG tensor is oriented differently from all of the other cases discussed: V_{11}, the most distinct component, is aligned close to the Cl···HO bond ($\angle(V_{11}-\text{Cl}-\text{H}) = 24.4°$), and V_{22} is near the Cl···HN bond ($\angle(V_{22}-\text{Cl}-\text{H}) = 13.0°$). Not only is the value of V_{33} reduced in comparison to the other systems but also the theoretically determined sign of V_{33} is observed to be opposite, which is consistent with V_{33} being oriented approximately perpendicular to the NH···Cl···HO plane.[67] As further experimental and theoretical ^{35}Cl NMR data are accumulated for well-characterized HCl pharmaceuticals, it is anticipated that ab initio

(67) Tang, J. A.; Ellis, B. D.; Warren, T. H.; Hanna, J. V.; Macdonald, C. L. B.; Schurko, R. W. *J. Am. Chem. Soc.* **2007**, *129*, 13049.

calculations will play a major role in structural characterization of polymorphs.

Examination of the theoretical CS tensor parameters also reveals good general agreement with experimental data. There are no simple correlations between basic structural features and CS tensor parameters, with one exception: we note that, for PH and TH, the Euler angles indicate that V_{33} and the most shielded component of the CS tensor, σ_{33}, are nearly coincident, while, for LH and BH, the higher values of β indicate noncoincidence of these components (Figure S8). This is consistent with one short contact dominating the CS tensor components in the former cases and two short contacts resulting in a change in tensor orientation in the latter cases. Of course, a wider spread of complexes will be examined in a forthcoming study to increase our understanding of the relation of chlorine CSA to structure, since the origin of CS tensor parameters are somewhat more complex than those of the EFG tensor; nonetheless, these results show promise for future detailed structural investigations.

4. Conclusions

This study represents the first application of ^{35}Cl SSNMR for the structural characterization of and identification of polymorphism in solid pharmaceuticals. ^{35}Cl SSNMR spectroscopy is clearly a powerful complimentary technique to XRD and ^{13}C SSNMR experiments, providing clear information on the number of chlorine sites and showing great utility for identifying sites in noncrystalline, disordered or even impurity phases, especially in cases where the solid-state ^{13}C NMR spectra or powder XRD experiments cannot unambiguously differentiate polymorphs. The use of ultrahigh field NMR spectrometers is crucial for the success of such work, for both fast acquisition of high *S*/*N* NMR spectra and accurate determination of anisotropic quadrupolar and chemical shift parameters. The sensitivity of the ^{35}Cl EFG and CS tensor parameters to the chlorine chemical environment allows for prediction of the number of short hydrogen bonds around the Cl^- ion. Theoretically calculated chlorine EFG and CS tensors are in good agreement with experimental data and will help to improve the predictive abilities of the solid-state ^{35}Cl NMR experiments. Consideration of the tensor orientations in the molecular frames provides a deeper understanding of the correlation between NMR parameters and chlorine−hydrogen bonding environments in LAs and holds strong promise for application to a wide array of HCl pharmaceuticals and related systems.

Acknowledgment. R.W.S. thanks NSERC, the Ontario Ministry of Research and Innovation, the Canadian Foundation for Innovation, the Ontario Innovation Trust, and the University of Windsor (UW) for funding. H.H. thanks the Ministry of Training, Colleges and Universities for an Ontario Graduate Scholarship, and UW for a Tuition Scholarship. Erin Norton (UW) is acknowledged for her assistance in synthesizing the LH1 sample. Joel A. Tang, Aaron J. Rossini, Dr. Victor Terskikh, and Dr. Shane Pawsey are thanked for assistance in acquiring the ^{35}Cl NMR spectra of BH at the National Ultrahigh-field NMR Facility for Solids in Ottawa, Canada. Prof. Charles L. B. Macdonald (UW) is acknowledged for useful discussions regarding the XRD data. Peter Gor'kov and Dr. William Brey at the NHMFL are thanked for building the 3.2 mm MAS HX probe and the low-E rectangular-flat coil HX probe and making them available on the wide bore 900 MHz NMR spectrometer in Tallahassee, Florida.

Supporting Information Available: Complete ref 51, additional NMR spectra and simulations, powder XRD data, and additional EFG tensor calculations, as well as experimental details and cif files (CCDC 673811−673813, 683735). This material is available free of charge via the Internet at http://pubs.acs.org.

JA802486Q